

ARTICLES

Sponge Model for the Kinetics of Surface Thermal Decomposition of Microcrystalline Solids: Application to HMX**Jack Simons***Chemistry Department, University of Utah, Salt Lake City, Utah 84112**Received: October 27, 1998; In Final Form: July 15, 1999*

A microscopic model is developed to describe the kinetics of thermal decomposition of microcrystals taking place on the crystals' surface, and the model is used to interpret certain experimentally observed decomposition rate (and product-formation) data of high-energy crystalline materials such as solid HMX. This so-called sponge model does not invoke autocatalytic steps yet is consistent with phenomenologically observed rate laws that display rapid rate enhancements early in the decomposition process. Its most essential assumptions are that (1) a molecule on the surface of a microcrystal undergoes unimolecular decomposition to form products (mainly gases) that promptly vacate the neighborhood of the just-decomposed molecule and (2) a molecule lying within the microcrystal (i.e., not on its surface) experiences packing forces from the surrounding crystal molecules that essentially prohibit its unimolecular decomposition. These assumptions, when incorporated into a kinetic model, allow the microcrystals to develop a spongy character (which the experimental data display) as their surface molecules decompose and expose underlying solid material thus generating new reactive molecules as the surface-area-to-volume ratio grows. It is this growth in surface area that produces the rate enhancement in the microcrystals' early stages of decomposition.

I. Introduction

In this paper, we put forth a microscopic model describing the thermal decomposition of microcrystals assumed to take place by unimolecular decay of molecules lying on the surfaces of the crystals. For simplicity, the size distribution of the microcrystals is assumed to be nearly monodispersed and to have three similar linear dimensions (thus to apply to nearly spherical or cubic crystals but not long needlelike crystals). Generalizations of this model to include distributions of microcrystal sizes and shapes are feasible, but the present development is limited to the specified cases to be well suited to the thermal decomposition of HMX that motivated its development.

In the design of the sponge model, two primary experimental observations weighed heavily, electron micrographs showing the temporal evolution in microcrystal morphology as thermal decomposition takes place and reaction rate data (both reactant mass loss and product mass gain) plotted vs extent of reaction. In the microscopy experiments,¹ the average diameters of microcrystals that were $180 \pm 48 \mu\text{m}$ prior to thermal treatment reduced to $166 \pm 45 \mu\text{m}$ after decomposition that produced 56% reactant mass loss. Hence, decomposition does not lead to proportional decrease in crystal size but, instead, primarily to crystal porosity. Figure 1 shows micrographs¹ of three selected microcrystals at various stages of decomposition.

It should be stressed that the decomposition of HMX microcrystals does not appear to take place via layer-by-layer loss of surface molecules, which would produce a monotonic decrease in crystal size as time evolves. Rather, decomposition occurs via the appearance of a highly pitted, spongy, porous

structure. It is for this reason that it would be inappropriate to use an "onion peeling" kinetic model analogous to that used by Eyring and co-workers² to treat radial inward burning of solid fuels. In the radial burning model, the outer surface of the solid is consumed before any of the material in inner layers can react; this is clearly inconsistent with the small change (180 to 166 μm) in average crystal radius and the evolution of spongy structure observed in HMX. Therefore, we have developed an entirely different model that we present in this paper. Specifically, we offer a kinetic model that is different from the shrinking-sphere model and which is consistent both with the qualitative features of HMX crystal morphology change (i.e., the evolution of spongy character) as well as the quantitative features of the experimentally observed^{3–5} rate of decomposition of HMX crystals and rate of appearance of product species.

A. Surface Thermal Decomposition of HMX: What Aspects We Address and Which We Do Not. The chemical structure of the explosive HMX is shown in Figure 2. As noted earlier, HMX appears to exist, in its most commonly used form, as a solid consisting of microcrystals whose three linear dimensions L_x , L_y , and L_z have similar magnitudes (see Figure 1 and Figure 1 of ref 3b). After being heated at temperatures of 220–250 °C in the absence of oxidizing substances and under conditions that sweep away (using N_2 flow gas) nascent gaseous products, this material decomposes to produce various gaseous products (mainly HONO, HCN, N_2O , and H_2CO and products of their subsequent reactions) as well as a nonvolatile residue (NVR) consisting mostly of polyamides. During such a thermal decomposition process, the microcrystals appear to evolve into "spongy" highly porous structures (see Figure 1b and also Figure

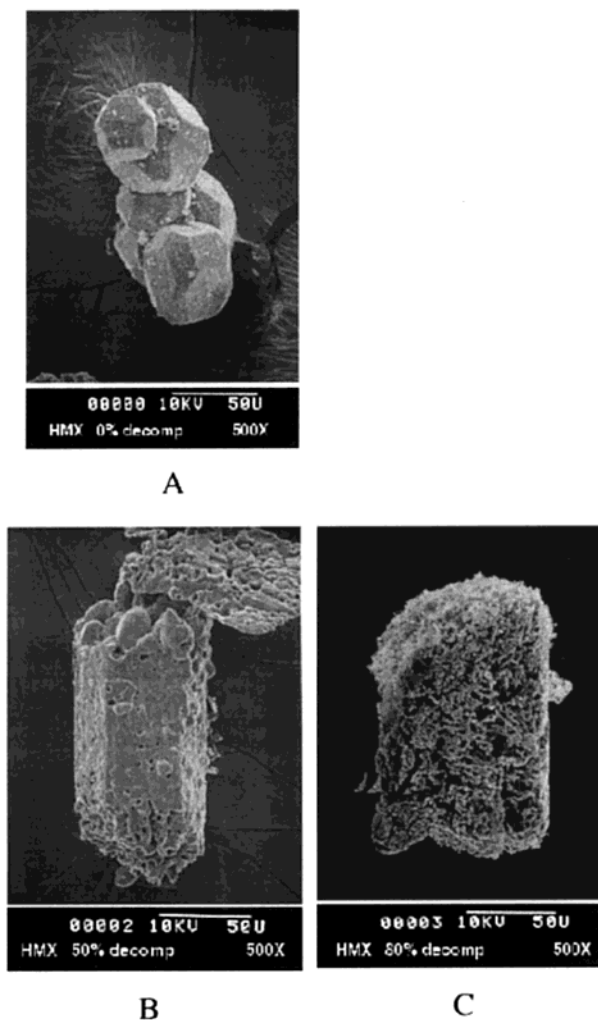


Figure 1. (a) Micrographs¹ of HMX microcrystals of dimension $\approx 40 \mu\text{m}$ prior to thermal treatment. (B, C) Micrographs¹ of two HMX microcrystals of dimension $\approx 80 \mu\text{m}$ after thermal treatment adequate to produce 50% (B) and 80% (C) decomposition within the total sample mass. The microcrystals shown in (C) and in (A) are not the same crystals; that is, they are three separate crystals. Their shapes offer some idea of the dispersion within an experimental sample. Their sizes are less than the average size within the sample (ca. $180 \mu\text{m}$) because higher quality micrographic pictures could be obtained of somewhat smaller crystals.

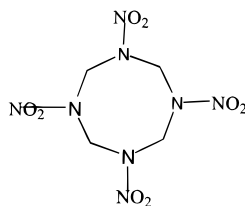


Figure 2. Chemical structure of HMX, whose surface thermal decay is suggested to undergo unimolecular decomposition initiated by N–NO₂ bond rupture. The melting point of HMX is $\approx 278 \text{ }^\circ\text{C}$.

1 of ref 3b) whose overall dimensions are not much different from the initial L_x , L_y , L_z . As noted above, these observations about the shapes and morphology changes accompanying thermal decomposition are essential to our development of the microscopic model detailed in this paper.

The decomposition of HMX as a function of temperature, pressure, and other reaction conditions and the subsequent reactions of species formed in the initial reaction step among themselves and with remaining HMX are extremely complicated

problems. At high pressures and under conditions of strong confinement, secondary reactions involving gaseous species produced in earlier reaction steps come into play because these gases are confined rather than swept away. At higher temperatures, the net reaction rate may be fast enough to render temperature control (e.g., keeping T constant) nearly impossible. Moreover, the finite thermal conductivity of the HMX crystal can give rise to strong temperature gradients within the crystal and can cause molecules within (i.e., not only on the surface) to decompose. All of these complicating features render the experimental parameters of such highly reactive and explosive materials difficult to control. This, in turn, makes the interpretation of the experimental data and theoretical modeling fraught with problems. In ref 5 is given an excellent survey of how various rate data can give rise to a wide range of activation energies (E^*) and preexponential factors (A) which, through kinetic compensation, all are consistent with measured rates. In ref 4, HMX reactions that occur in the solid, liquid, and gas phases are addressed and an excellent overview of what is thought about how HMX decomposes under various conditions is offered. And, as noted earlier, in ref 3, a wealth of data showing the time evolution of various products of HMX decomposition is given.

Although many of the issues treated in refs 3–5 are of fundamental importance to achieving a full picture of all the reactions involved in HMX's decay to its final, most stable, product species, in this paper we are by no means attempting to address all of them. Because of the daunting complexity of the full kinetics scheme, we decided to focus on modeling a limited set of experimental data for which the control of temperature seems to be reasonably in hand and for which the accumulation of gaseous products is unlikely to produce high pressures (and thus domination of secondary reactions). Specifically, we offer a model of the thermal decay of surface molecules to produce initial products (i.e., not products of subsequent reaction steps) that promptly vacate the decay site. Before describing our model, it is helpful to briefly review findings from three laboratories that have played especially important roles in characterizing the decomposition kinetics of HMX. We stress that our model is focused on decomposition taking place on the crystal surface and is aimed at reproducing the morphology changes and rate-vs-fraction decomposition data that characterize many experimental findings.

In 1996, Tarver et al.⁴ proposed a three-step model for the thermal decomposition of HMX in which (a) HMX undergoes unimolecular C–N and N–N bond breaking (with activation energy $E^* = 52.7 \text{ kcal/mol}$ and preexponential factor $A = 1.4 \times 10^{21} \text{ s}^{-1}$) to form methylene nitramine H_2CNNO_2 followed by (b) weakly exothermic unimolecular decomposition of these fragments to yield $\text{H}_2\text{CO} + \text{N}_2\text{O}$ or $\text{HCN} + \text{HNO}_2$ (with $E^* = 44.1 \text{ kcal/mol}$ and $A = 1.6 \times 10^{16} \text{ s}^{-1}$), followed by (3) very exothermic bimolecular gas-phase reactions to produce N_2 , H_2O , CO_2 , CO , etc. (with $E^* = 34.1 \text{ kcal/mol}$ and $A = 1.6 \times 10^{12} \text{ s}^{-1}$). The various activation energies and A factors were extracted from measurements carried out under various gas-confinement conditions (i.e., for step a at low confinement such that secondary gaseous reactions do not dominate, for step b at higher gas confinements, and for step c using gas-phase rate data on the species produced in step b as they react to produce the very stable species of step c). If this picture of HMX decomposition were complete, one would expect that activation energies and A factors extracted from experimental probes carried out as a function of the extent of crystal decomposition would decrease as the extent of reaction varies, and the

activation energy and A factor observed in the early stages of reaction should be close to $E^* = 52.7$ kcal/mol and $A = 1 \times 10^{21}$ s⁻¹.

A wide range of experimental data have been interpreted by Behrens et al.³ in terms of a model in which solid HMX undergoes induction, acceleratory, and decay stages and thus is suggested to involve an autocatalytic reaction mechanism. The initial decay of HMX is thought to produce a catalytic intermediate which then lowers the activation barrier to subsequent thermal decomposition and causes the reaction to accelerate. Again, if this model were fully correct, one would expect the measured activation energy to be high in early stages of decomposition and to decrease as the reaction accelerates.

In 1994, Brill et al.⁵ offered an insightful overview of the state of affairs having to do with the measured activation energies and A factors for HMX (solid, liquid, and gas) decomposition. That article points out that a very wide range of E^* and A values have been reported, which makes it difficult to know which values relate to which steps in the complex series of reactions that certainly give rise to the transformation of HMX ultimately to N₂, H₂O, CO₂, CO, and NVR.

Wight and co-workers have measured initial decomposition rates¹ and obtained an activation energy of 35 ± 3 kcal/mol. This particular activation energy (35 kcal/mol), which is used in the present simulations, lies within the range of the values discussed in ref 5, but it should be stressed that this specific choice has little or no effect on the sponge model's ability to duplicate the "shape" of the experimental rate-vs-fraction decomposition data or the changes in crystal morphology that accompany decomposition. Only the absolute magnitude of the rates depend on the choice of activation energy; the characteristic shape of these rate plots (see, for example, Figures 4 and 6 in ref 3b where a large number of such plots are displayed) do not depend on E^* or A .

To summarize, the sponge model put forth in this paper focuses on the unimolecular decomposition of solid-state HMX molecules lying on the surface of the microcrystals and *not* on any subsequent reactions of gas or solid species formed after the first unimolecular step. Such a model produces a functional form for the rate of HMX decomposition vs fraction decomposition α that (a) agrees well with the multitude of such plots displayed, for example, in Figures 4 and 6 of ref 3b, (b) displays rate acceleration for small α and rate decay for large α without introducing any autocatalytic steps, and (c) uses one set of E^* and A values that remain constant as ranges from 0 to 1.0. Moreover, the model explains the spongy morphology of the crystals (see, for example, Figure 1 and Figure 1 of ref 3b) that develops as decomposition occurs.

B. An Empirical Rate Law That Has Been Used To Fit Rate Data. The rate of loss of reactant HMX molecules, probed as the rate of total mass loss of a sample containing many microcrystals, has been examined experimentally and found empirically to fit a rate expression of the form⁶

$$\text{rate} = k \alpha(1 - \alpha) \quad (1)$$

where α is the degree of decomposition, ranging from $\alpha = 0$ at $t = 0$ to $\alpha = 1$ as $t \rightarrow \infty$, and the rate is expressed in terms of the rate of change in α . Many examples of such rate measurements for HMX and their plots vs α are shown in Figures 4 and 6 of ref 3b. The essential features of these plots are rates that rise rapidly to a maximum (usually below $\alpha = 0.5$) and then fall more slowly toward zero. It should be noted that eq 1 predicts a maximum rate at $\alpha = 0.5$, whereas the data of, for example, ref 3 show maximum rates for $\alpha < 0.5$. Hence, there

is reason to believe that the rate expression of eq 1 is not entirely correct; as will be seen shortly, the sponge kinetic model put forth here gives (from first principles, not by assumption) a rate law similar to eq 1 but skewed such that the peak rate occurs for $\alpha < 0.5$.

C. Rate Parameters A and E^* . In carrying out the simulations whose results are reported below, we employed a rate coefficient $k = A \exp(-E^*/RT)$ with an activation energy of 35 ± 3 kcal/mol for HMX and an A factor of $A = 1 \times 10^{12}$ s⁻¹. The value $E^* = 35 \pm 3$ kcal/mol is in the range known for the dissociation energy of the N–NO₂ bond that may be the first bond broken in HMX's decomposition.⁷ As noted earlier, the particular choice of E^* and A parameters does not affect how the sponge model duplicates the shapes of the rate-vs- α plots or the evolution of spongy character in the microcrystals; these parameters only affect the absolute values of the computed rates.

D. Basic Assumptions of Our Microscopic Model. In this paper, we offer a molecule-level microscopic model whose predictions (a) are consistent with the visually observed morphology changes in microcrystalline HMX illustrated in Figure 1 and the shape of the rate profile graphs shown in Figures 4 and 6 of ref 3b and (b) does not require the introduction of any bimolecular or autocatalytic mechanism. We term this the "sponge model" because of the observed porous, spongy nature taken on by the HMX crystals as they decompose.

This model uses a lattice description of the HMX molecules' local environment and expresses the rate of loss of HMX molecules in terms of (a) a unimolecular rate coefficient k having a fixed E^* value and a fixed A factor and (b) the number of "active" HMX molecules at any time t during the thermal decomposition.

An active HMX molecule is defined as one with at least one of its four N–NO₂ units not surrounded by other crystalline HMX molecules, and it is assumed that only these active molecules are able to undergo unimolecular decay to produce nascent gases and NVR. This model thus assumes that crystal packing forces provide sufficient hindrance to inhibit the decomposition process and that, until this hindrance is relieved by loss of at least one of the surrounding crystal HMX molecules, further decay of the crystal cannot proceed.

At the beginning of a microcrystal's decay, only its surface HMX molecules are active because only they can have N–NO₂ groups exposed. However, as surface molecules decompose and uncover HMX molecules in underlying crystal layers, thus generating pits that lead to pores throughout the microcrystal, these underlying crystal molecules can become active. According to our model, it is the erosion of underlying layers (N.B., *not* in a layer-by-layer manner characteristic of Eyring's shrinking-sphere model) that ultimately leads to the spongy porous nature of the decomposing HMX, and *it is the change in surface area-to-volume ratio* accompanying increased porosity that causes the increase in active molecules and thus *the acceleration in decomposition rate as time proceeds*.

II. Description of the Sponge Model and Its Rate Law

A. Microcrystal Size and Shape. We begin by modeling a macroscopic sample of solid HMX as consisting of N identical microcrystals each of which contains n_0 HMX molecules and each of which is (nearly) cubic with volume v_0 . Clearly, Nv_0 is the total volume of such a sample (ignoring the space occupied by voids and cracks), Nn_0 is the total number of HMX molecules it contains, $6(v_0)^{2/3}$ is the initial surface area of each microcrystal, $(Nv_0/Nn_0) = v_0/n_0$ is a "molecular volume" characteristic of the

compound HMX and its crystal structure, and N depends on the initial granularity of the HMX sample.

It should be stressed that we do not consider build up of gaseous products surrounding the HMX microcrystals; once an HMX molecule undergoes N–NO₂ bond rupture, it is assumed to have produced whatever (intermediate or final product) gases and NVR species it generates with the gases assumed to have vacated the neighborhood of the just-decomposed HMX molecule. Thus, issues of what goes on in the spaces between microcrystals, within cracks or voids inside microcrystals, and in the gas surrounding the sample are ignored in our treatment.

B. Active Molecules and Crystal Packing Geometry. We view the crystalline packing of the HMX molecules in the following terms: (a) Each molecule lying totally *within* the crystal (i.e., not on the surface) is surrounded by near-neighbor HMX molecules that offer sufficient crystal packing forces to render unimolecular decomposition impossible because none of its four N–NO₂ bonds is capable of rupturing (except under very high-energy conditions). (b) Not all of the surrounding molecules provide direct contact with an N–NO₂ group of a given HMX molecule, so the number of nearest neighbors is *not* equal to the number of N–NO₂ bonds that are inhibited. For example, in HMX, there are four equivalent N–NO₂ bond sites per HMX molecule, but there are more than four nearest neighbors (depending on the crystal phase one is in) to a given HMX molecule. (c) We denote by C the number of N–NO₂ bonds that can be inhibited by neighbor HMX molecules, and we use D to label the number of nearest neighbor molecules each HMX has *within* the crystal. Clearly, D will be larger than C , and for HMX, C is 4.

A *surface* HMX molecule may have fewer than C molecules surrounding its N–NO₂ bonds. Such surface molecules form the initial ($t = 0$) members of the species deemed *active* in our model (i.e., we assume that any molecule surrounded by a full set of C bond-blocking neighbors experiences sufficient inhibition of its N–N bond stretching to prevent breaking of any such bond). For a crystal that has not yet undergone any decomposition, there would be

$$n_{\text{act}}(t = 0) = 6n_0^{2/3} \quad (2)$$

active molecules because only the surface molecules (there are $6n_0^{2/3}$ of them if the microcrystal is viewed as consisting of n_0 cubic molecules each with volume v_0/n_0 that exist on the surface of area $6v_0^{2/3}$) are active for the initial crystalline material.

C. Unimolecular Decomposition Rate for an Active Molecule. A *fundamental assumption* of our model is that any HMX molecule surrounded by C blocking neighbors cannot undergo N–N bond rupture initiated decomposition and any HMX molecule surrounded by fewer than C neighbors blocking its N–N bond sites will decompose at a rate characterized by a unimolecular rate coefficient

$$k = A \exp(-E^*/RT) \quad (3)$$

It should be noted that we do not incorporate any influence of the crystal packing on either the activation energy E^* or the unimolecular A factor (i.e., we use an E^* and A which are consistent with N–NO₂ bond energetics of isolated HMX molecules). In other words, the decay of an HMX molecule at one site is assumed to have no energetic or A -factor influence over HMX molecules at other sites, except that decay of the first molecule may expose N–NO₂ groups of other molecules that had previously been surrounded by C blocking neighbors.

D. Development of the Sponge Kinetics Equations. Early in the thermal decay of each microcrystal, its surface HMX molecules are the only active molecules, so the initial rate of loss of HMX will be proportional to $6kn_0^{2/3}$ per microcrystal or $6Nkn_0^{2/3}$ for the entire sample. However, as the surface molecules begin to erode, molecules in the underlying layers begin to become exposed in the sense that they no longer are surrounded by C blocking neighbors. As the crystal thus undergoes further decomposition, more and more of its HMX molecules find themselves activated as they lose one or more of their C blocking neighbors. Eventually, all of the remaining molecules have become active and remain so until all molecules have decomposed.

To formulate this decay in terms of a set of kinetics equations, we consider the active molecules within the HMX crystal at a time t , and we ask how many active molecules will decay and how many new active molecules will be formed in a time interval dt :

$$\frac{dn_{\text{act}}(t)}{dt} = -kn_{\text{act}}(t) + \text{rate of creation of new active molecules} \quad (4)$$

The *rate of loss* shown in the above kinetic equation is simply the unimolecular decay rate kn_{act} and is assumed to have $k = A \exp(-E^*/RT)$ with E^* near 35 kcal/mol and A near $1 \times 10^{12} \text{ s}^{-1}$. For the *rate of creation* of new active molecules, we note that each time an HMX molecule undergoes unimolecular decay and the products of this decomposition promptly leave as gases or form NVR, it vacates a lattice site. This newly vacated lattice site (let us label it S_0) has the *potential* for creating new active HMX molecules that had been blocking neighbors to this site. Whether it realizes this potential depends on the instantaneous local crystal packing situations of the neighbor sites.

a. Average-Environment Approximation. Probably the most *significant approximation* of our model is made as we describe the instantaneous (i.e., at any time t in the decomposition process) environment of any *particular* HMX molecule site in terms of an “average environment” formed by averaging over the instantaneous environments of *all* HMX molecules⁸ remaining in the sample. Specifically, the S_0 HMX molecule that has just disappeared had $C - 1$ blocking neighbors (let us label them S_1 through S_{C-1}). The probability (this is where the “average” aspect of our model enters) that any one of the $C - 1$ sites S_1 through S_{C-1} contains an HMX molecule is $n(t)/n_0$ (i.e., the fraction of HMX molecules remaining at time t). However, even if a site S_k ($k = 1, 2, \dots, C - 1$) is occupied, its HMX molecule will be a *new* active molecule only if *all* C blocking sites surrounding S_k had been occupied prior to decay of the HMX molecule in S_0 . We know that one site (i.e., S_0 itself) surrounding S_k was occupied, but what about the remaining $C - 1$ sites? Again, we assume these sites are each occupied with an average probability of $(n(t)/n_0)$, so the probability that all $C - 1$ blocking neighbor sites of S_k are occupied after the molecule at S_0 decomposes is $(n(t)/n_0)^{C-1}$. Combining these assumptions about the instantaneous environment of an HMX molecule that has just undergone unimolecular decay, we can write the net rate of change of active HMX molecules as

$$\frac{dn_{\text{act}}(t)}{dt} = -kn_{\text{act}}(t) + kn_{\text{act}}(t)(C - 1)(n(t)/n_0)(n(t)/n_0)^{C-1} \quad (5)$$

b. Kinetics Equations for Loss of HMX. Within this kinetic model, the total rate of loss of HMX molecules per microcrystal is given by

$$dn(t)/dt = -kn_{\text{act}}(t) \quad (6)$$

The total rate of loss of reactant molecules is given as

$$dn_{\text{tot}}/dt = Ndn/dt \quad (7)$$

This set of coupled kinetic equations (eqs 5 and 6) express the sponge model and are to be solved subject to the initial conditions: $n_{\text{act}}(t = 0) = 6n_0^{2/3}$ and $n(t = 0) = n_0$.

III. Examination of Sponge Model Kinetics at Short and Long Times

Let us begin by considering the equation for the rate of change of the number of active molecules. The expression for dn_{act}/dt contains a negative first and a positive second term. The two terms combine at short times (when $n(t)/n_0 \approx 1$) to produce a net positive rate

$$dn_{\text{act}}/dt = k(C - 2)n_{\text{act}} \quad (8)$$

while, at long times (when $n(t)/n_0 \ll 1$), the first term dominates to produce a net negative rate

$$dn_{\text{act}}/dt = -kn_{\text{act}} \quad (9)$$

This observation is at the heart of understanding why the rate of decomposition of an HMX sample has the shape shown in Figures 4 and 6 of ref 3b.

A. Short-Time Kinetics. The solution to the short-time equation for n_{act} , subject to the initial condition $n_{\text{act}}(t = 0) = 6n_0^{2/3}$ is

$$n_{\text{act}}(t) = 6n_0^{2/3} \exp[(C - 2)kt] \quad (10)$$

Using this result for n_{act} in the equations for $dn(t)/dt$ gives

$$n(t) = n_0 - (6n_0^{2/3}/(C - 2))[\exp[(C - 2)kt] - 1] \quad (11)$$

Notice that the sponge model predicts that n_{act} should grow and n should decrease exponentially with time and with equal short-time exponential rate coefficients given by

$$k_{\text{short-time}} = (C - 2)k \quad (12)$$

Notice also that the rate of loss of reactants dn/dt and the fraction of reactant molecules that have decomposed α can be related since

$$-dn/dt = k6n_0^{2/3} \exp[(C - 2)kt] \quad (13)$$

and

$$\alpha = 1 - n(t)/n_0 = (6n_0^{-1/3}/(C - 2))[\exp[(C - 2)kt] - 1] \quad (14)$$

so

$$-dn/dt = kn_0(C - 2)\alpha + k(6n_0^{2/3}) \quad (15)$$

The latter result states that the rate when plotted versus the fraction α should begin, near $\alpha = 0$ or $t = 0$, at a value $k(6n_0^{2/3})$ corresponding to the rate of decay of the surface species only. The rate should then *grow linearly with α* but *with a slope equal to $kn_0(C - 2)$* ; this slope reflects the number of newly activated molecules that accompany thermal decomposition of one HMX molecule through the $n_0(C - 2)$ factor (i.e., one HMX molecule is lost, but $C - 1$ new active HMX molecules are created).

The expression giving α as a function of time suggests that α should initially grow exponentially with time from $\alpha = 0$ at $t = 0$ and with an exponential coefficient of $(C - 2)k$. The development to follow shows that $d\alpha/dt$ should pass through a maximum and return to zero with a long-time exponential falloff coefficient of k .

B. Approximately When Will the Rate Maximize? Before moving on to consider the long-time solutions to the kinetic equations and how to “connect” the short- and long-time expressions, it is interesting to ask at what time t^* will n_{act} equal n when both are approximated by their short-time expressions. This time, and the value of n_{act} at that time, are expected to offer important characterizations of the material when the rate of decomposition is highest. Setting $n_{\text{act}}(t)$ equal to $n(t)$ produces

$$\exp[(C - 2)kt^*] = [1/6n_0^{1/3} + 1/(C - 2)]/[1 + 1/(C - 2)] \approx 1/6n_0^{1/3}(C - 2)/(C - 1) \quad (16)$$

for the equation giving t^* in terms of C , k , and the initial number of molecules, n_0 . The number of active molecules existing at t^* is

$$n_{\text{act}}(t^*) = n_0(C - 2)/(C - 1) = n(t^*) \quad (17)$$

the fraction reacted at this time, $\alpha(t^*) = 1 - n(t^*)/n_0$, is given by

$$\alpha(t^*) = 1/(C - 1) \quad (18)$$

and the rate of loss of reactants at t^* is

$$-dn/dt = kn_{\text{act}}(t^*) = kn_0(C - 2)/(C - 1) \quad (19)$$

Most of the rate vs α data shown in Figures 4 and 6 of ref 3b for HMX seem to peak below $\alpha = 0.5$, which would imply a C value of above 3, in line with earlier remarks about steric effects in HMX's four equivalent N-N bonds for which C should be 4. The expression for the rate at t^* suggests that most (because $(C - 2)/(C - 1) = 2/3$) of the initial molecules become activated within the time t^* . The expression for $\alpha(t^*)$ suggests that the percent decomposition at the peak rate should be independent of k , sample size, and crystal size, and should depend only on crystal packing factors (through $1/(C - 1)$). However, the time t^* required to reach the peak rate should depend also depend on k and n_0 . These predictions can and should be subjected to further experimental tests.

C. Long-Time Kinetics. Returning to the sponge kinetics equations and considering the equation for n_{act} at times long enough for the ratio $(n(t)/n_0)^{C-1}$ to be neglected compared to unity, one arrives at

$$dn_{\text{act}}/dt = -kn_{\text{act}} \quad (20)$$

which has the solution

$$n_{\text{act}}(t) = n_{\text{act}}(t') \exp[-k(t - t')] \quad (21)$$

where t' is some (long) time for which n_{act} is known. Notice that the exponential decay of n_{act} at long times is predicted by the sponge model to occur with a rate coefficient

$$k_{\text{long-time}} = k \quad (22)$$

that is *not identical* to the rate coefficient $k_{\text{short-time}} = (C - 2)k$ characterizing the short-time growth. So, n_{act} is expected to grow

rapidly to its maximum value of ca. $n_0(C - 2)/(C - 1)$ near t^* and to subsequently decay more slowly from then on.

D. Connecting the Short and Long Times. To connect the long-time solution for n_{act} to the short-time solution, one would have to have in-hand an analytical expression of n_{act} that is valid at short, intermediate, and long times. We do not know of such a solution (N.B., the equations for n_{act} and n are coupled and that for n_{act} is highly nonlinear because of the $(n(t)/n_0)^{C-1}$ factor). Therefore, we choose to use the time at which all of the remaining molecules are expected to be active to (approximately) connect our short- and long-time kinetics. Explicitly, we take $t' = t^*$ and $n_{\text{act}}(t') = n_{\text{act}}(t^*) = n(t^*) = n_0(C - 2)/(C - 1)$, which then produces

$$n_{\text{act}}(t) = n_0(C - 2)/(C - 1) \exp[-k(t - t^*)] \quad (23)$$

at long times. Using this result for n_{act} in the kinetic expressions for $dn/dt = -kn_{\text{act}}$ produces the following:

$$n(t) = n(t^*) \exp[-k(t - t^*)] = n_0(C - 2)/(C - 1) \exp[-k(t - t^*)] \quad (24)$$

These (approximate) equations predict that n_{act} and n should decay with identical rate coefficients $k_{\text{long-time}} = k$.

Again, it is possible to express the rate of loss of reactant molecules in terms of the percent decomposition at long times by using

$$-dn/dt = kn_{\text{act}} = kn_0(C - 2)/(C - 1) \exp[-k(t - t^*)] \quad (25)$$

and

$$1 - \alpha = (C - 2)/(C - 1) \exp[-k(t - t^*)] \quad (26)$$

so

$$-dn/dt = kn_0(1 - \alpha) \quad (27)$$

for long times and hence as α approaches unity. These results suggest that a plot of the rate of loss of reactant vs α should have a slope of $-kn_0$ at long times. Recall that the slope of such a plot at short times is expected to be $kn_0(C - 2)$. The HMX rate vs α data plotted in Figures 4 and 6 of ref 3b seem to show this behavior; the slope at small α is steeper than that as α approaches unity.

E. Full Numerical Integration of the Kinetics Equations.

a. A Specific Example. In Figure 3 are shown simulated rates obtained by numerically solving the full sponge kinetics equations detailed in section II.D.b using an activation energy $E^* = 35$ kcal/mol, a preexponential factor of $A = 1 \times 10^{12}$ s $^{-1}$, and a number of blocking neighbors of $C = 4$. The rate is reported in terms of $d\alpha/dt$ vs the fraction decomposition α .

For this particular simulation, an initial microcrystal size corresponding to 10^6 HMX molecules, of which 6×10^4 are initially on the surface, was used. Assuming a nearest-neighbor spacing of ca. 8 Å, as in HMX, this corresponds to a microcrystal of only 800 Å on a side, much smaller than the microcrystals used in the experiments. Nevertheless, the solution of the sponge kinetic model shown in Figure 3 possesses features much like those of the experimental rate data given in Figures 4 and 6 of ref 3b. In particular, the rate clearly shows an acceleration at short time and a slower falloff at long time. Moreover, the fraction decomposition at which the maximum rate is reached is similar to what is seen experimentally.

b. Improvement in Treating the Independent Blocking Neighbors. In the numerical solution of the full kinetic equations (eqs

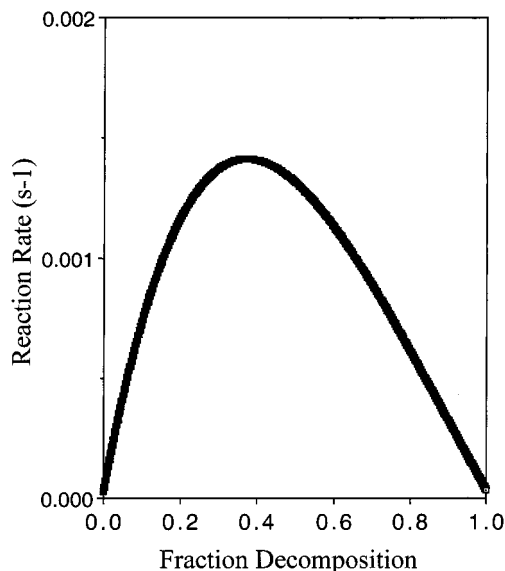


Figure 3. Simulated rate of decomposition of HMX at $T = 250$ °C obtained by numerical integration of the sponge kinetics equations.

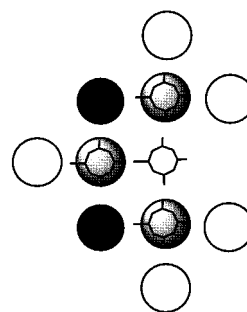


Figure 4. Representation of the local environment around an HMX molecule that has one of its N-NO $_2$ bonds activated.

5 and 6), the term $kn_{\text{act}}(t)(C - 1)(n(t)/n_0)(n(t)/n_0)^{C-1}$ giving the rate of gain of active HMX molecules has been altered to achieve a somewhat more quantitatively correct result. Recall from section II.D.a that $(C - 1)(n(t)/n_0)$ is the number of remaining blocking neighbor sites $(C - 1)$ times the probability $(n(t)/n_0)$ that such a site is occupied by an HMX molecule. Then $(n(t)/n_0)^{C-1}$ is supposed to give the probability that all of these $C - 1$ remaining blocking neighbor sites are also surrounded by a full complement of blocking HMX molecules. The problem is that using the factor $(n(t)/n_0)^{C-1}$ assumes independent probabilities that each of the remaining blocking molecules has its surrounding sites occupied; this independent probability assumption is not correct as we now attempt to demonstrate using Figure 4.

In Figure 4, the central HMX molecule clearly has one of its N-NO $_2$ bonds exposed and hence activated; its $C - 1 = 3$ remaining N-NO $_2$ bonds are blocked by the lightly shaded neighbor HMX molecules. Each of these 3 lightly shaded blocking neighbors possesses 3 blocking neighbor sites of its own (the dark and unshaded sites) plus a fourth neighbor (the central HMX). Hence, one might think there are $3 \times 3 = 9$ sites that neighbor the three lightly shaded HMX molecules. However, there are only 7 distinct sites because some (the dark sites) serve as potential blocking neighbor sites to more than one lightly shaded HMX. So, averaged over the three blocking neighbors to the central HMX, each of the lightly shaded sites has only $(7/9)(C - 1) = 7/3$ independent surrounding potential blocking sites.

For these reasons, we replaced the form of the expression $kn_{\text{act}}(t)(C-1)(n(t)/n_0)(n(t)/n_0)^{C-1}$ giving the rate of formation of active HMX species by $kn_{\text{act}}(t)(C-1)(n(t)/n_0)(n(t)/n_0)^{(C-1)(7/9)}$ when carrying out the numerical simulations whose data are displayed above. This correction is made to more properly calculate the probability that each of the $C-1$ blocking neighbors to a just-decomposed molecule will have all $C-1$ of its remaining neighbor sites occupied. Clearly, the precise form of the correction factor introduced here will depend on the particular crystal packing environment that arises in the material under study. For HMX, we believe that the $7/9$ statistical scaling has a clear basis. When the sponge model is applied to other materials, knowledge of how that material is packed in the crystal as well as of how many blocking neighbors are present must be in hand.

F. Overview of Short- and Long-Time Behavior. In summary, data on the rate of loss of HMX molecules when graphed vs the fraction decomposition α should (1) begin (at $\alpha = 0$) with a nonzero initial rate of $6kn_0^{2/3}$ corresponding to the rate due to the decomposition of surface molecules and (2) grow with an initial slope of $kn_0(C-2)$ (3) until a peak rate of magnitude $kn_0(C-2)/(C-1)$ is reached (4) at a value of $\alpha = 1/(C-1)$, after which (5) the rate should decay until α approaches unity near which the graph has a slope of $-kn_0$.

IV. Overview and Predictions of the Sponge Model

A. Working Equations. The sponge model describes the thermal decomposition of solids consisting of symmetrical microcrystals in terms of (a) a single unimolecular decay rate coefficient $k = A \exp(-E^*/RT)$, (b) a crystal packing dependent number of N-N bond blocking neighbors C , and (c) an initial number $6n_0^{2/3}$ of active surface molecules characteristic of the initial surface area-to-volume ratio of the crystals.

This model yields for *short times*

$$n_{\text{act}}(t) = 6n_0^{2/3} \exp[(C-2)kt] \quad (10)$$

$$n(t) = n_0 - (6n_0^{2/3}/(C-2))[\exp[(C-2)kt] - 1] \quad (11)$$

and for *long times*

$$n_{\text{act}}(t) = n_0(C-2)/(C-1) \exp[-k(t-t^*)] \quad (23)$$

$$n(t) = n(t^*) \exp[-k(t-t^*)] = n_0(C-2)/(C-1) \exp[-k(t-t^*)] \quad (24)$$

The time t^* at which nearly all of the remaining molecules have become activated is given in terms of the rate coefficient k , the initial number of molecules n_0 , and C as

$$\exp[(C-2)kt^*] \approx {}^{1/6}n_0^{1/3}(C-2)/(C-1) \quad (16)$$

and this t^* allows the short-time and long-time expressions for n_{act} and n to connect at t^* .

B. Predictions of the Model. The set of equations given above predict that n_{act} and hence the rate of decomposition of HMX should grow *rapidly* (with $k_{\text{short-time}} = (C-2)k$) until a time t^* after which n_{act} , the rate, and n should decay *more slowly* (with $k_{\text{long-time}} = k$). For large microcrystals (i.e., those having larger $n_0^{1/3}$), the time t^* where the maximum rate of decomposition occurs will be longer than for very fine microcrystals (with smaller $n_0^{1/3}$) although the fraction decomposition at the peak rate $\alpha(t^*) = 1/(C-1)$ will be the same independent of microcrystal size. These predictions of the sponge model should be subjected to experimental checks by carrying out series of thermal decomposition rate measurements using crystals of varying initial size.

Acknowledgment. This work has been supported by NSF Grant CHE-9618904 and by proceeds of the Henry Eyring Endowed Chair. The author wishes to acknowledge his friend and colleague Prof. C. A. Wight for interesting him in the problem addressed here.

References and Notes

- (1) The micrographs shown in Figure 1 were obtained from Prof. C. A. Wight at Utah and appear in: Lofy, P.; Wight, C. A. Thermal Decomposition of HMX Below Its Melting Point. *Proceedings of the JANNAF Combustion Subcommittee Meeting*; Tucson, AZ, 1998; Chemical Propulsion Information Agency, Johns Hopkins University: Baltimore, 1998.
- (2) Eyring, H.; Powell, R. E.; Duffey, C. H.; Parlin, R. B. *Chem. Rev.* **1959**, *45*, 16.
- (3) (a) Behrens, R., Jr.; Bulusu, S. *Mater. Res. Soc. Symp. Proc.* **1993**, *296*, 13. (b) Behrens, R. *J. Phys. Chem.* **1990**, *94*, 6706. (c) Behrens, R.; Mack, S.; Wood, J. Presented at the JANNAF Combustion and Hazards Meeting, Tucson, AZ, Dec 1998.
- (4) Tarver, C.; Chidester, S.; Nichols, A. *J. Phys. Chem.* **1996**, *100*, 5794.
- (5) Brill, T.; Gongwer, P.; Williams, G. *J. Phys. Chem.* **1994**, *98*, 12242.
- (6) A wide range of phenomenological rate laws are discussed in *Global Kinetic Analysis of Complex Materials* (Burnham, A. K.; Braun, R. L. *Energy Fuels*, submitted for publication) although no molecular-level mechanism is used to achieve the rate law form used here.
- (7) For an isolated HMX molecule, the lowest energy process for HMX decomposition is the N-NO₂ bond rupture which has an energy requirement of 35–40 kcal/mol. A less endothermic process involves elimination of HO-NO (via concerted N-N bond rupture, C-H bond rupture, and O-H bond formation); however, this process has a higher activation energy than N-NO₂ bond rupture. Finally, decomposition of isolated HMX into H₂-CNNO₂ is endothermic by 50–53 kcal/mol. No one knows for certain what energy is required to break the N-NO₂ bond within solid HMX. However, the model developed here assumes that only those crystalline HMX molecules that have one or more NO₂ group exposed (i.e., not completely surrounded by other molecules in the crystal) can react. Therefore, it is reasonable that the E^* appropriate to the cleavage of such N-NO₂ bonds should be close to the N-N bond energy for an isolated HMX molecule.
- (8) It is possible to circumvent the averaging approximation by using computer simulations to solve equations for the instantaneous survival probabilities of individual HMX molecules at each lattice site. However, our intent here is to offer an analytical model that may prove useful, even if more approximate, in understanding and analyzing the observed thermal decomposition rates of microcrystalline solids.